JOURNAL OF APPLIED ELECTROCHEMISTRY 26 (1996) 515–521

Active surface area in oxide electrodes by overpotential deposited oxygen species for the oxygen evolution reaction

J. C. K. HO, D. L. PIRON

Département de Métallurgie et de Génie des Matériaux, Ecole Polytechnique de Montréal, Case Postale 6079, succ. Centre-ville, Montréal, Québec, H3C 3A7 Canada

Received 15 March 1995; revised 28 August 1995

The electrochemical active surface area at oxide electrodes of Pt and electrodeposited Ni, Co and $Ni_{20}Co_{80}$ alloys was evaluated in 5 M KOH solutions based on the charge for electrochemical desorption of a monolayer of overpotential deposited oxygen (OPD O) species. The *in situ* technique employed for the charge measurement involves galvanostatic charging (OPD O) adsorption), followed by simple discharging (OPD O desorption) experiments. It is observed that surface area estimated by this new technique for the oxidized surfaces of the metals studied here are consistent with those from a.c. impedance spectroscopy. The activity of the metal towards the oxygen evolution reaction (OER) is also discussed in terms of their active surface area estimated in this study.

1. Introduction

It is well known that electrode activities depend on both the catalytic properties of the material and the electrode surface area. Yet, *in situ* electrode surface area determination has still remained one of the most difficult problems in electrochemical studies [1]. Traditionally, electrode surface area is estimated based on the measurement of double-layer capacitance, C_{dl}, which arises at all electrode-electrolyte interfaces [2, 3], using, for instance, a.c. impedance spectroscopy. Surface area obtained in this way is considered to be real because it can normally be related to the portion of electrode surface that is in contact with the electrolyte and thus available for faradaic reactions. However, this 'real' area might or might not be electrochemically active for the reaction of interest. Hence, for practical electrocatalyst evaluation, it is necessary to have experimental techniques that can provide accurate measurement of electrode surface area that is active only for a particular reaction. This allows for a more genuine comparison of electrode activity amongst different electrodes. Cyclic voltammetry could be considered as one such technique for the deposition of O, H and Pb species at noble metals (cf [3]) in the potential region between the cathodic hydrogen and the anodic oxygen evolution reactions (the so-called underpotential depositions, UPD of O, H and Pb). The charge estimated under the voltammetric adsorption peaks over a certain range of potential (e.g., 0.0–0.5 V vs RHE for UPD hydrogen at Pt) corresponded exactly to monolayer coverage of the electrode surface by the adsorbate, in the case of UPD hydrogen, H. Thus, if the charge required for 1 cm^2 of electrode surface is known, surface area active for the adsorption process can be estimated. This relatively simple procedure, however, can not be applied to many industrially important processes such as the Cl_2, F_2, H_2 and O_2 evolution reactions because the adsorption peaks for the reaction intermediate(s) are always obscured by the excessive gas evolution.

In our previous study [4], a new technique was devised for the determination of active electrode surface area at Pt and stainless steel electrodes in alkaline solutions using the charge corresponding to monolayer coverage of the electrode by the H intermediate in the hydrogen evolution reaction (HER). In this paper, this technique is extended to the measurement of active electrode surface area for the oxygen evolution reaction, demonstrably, on the oxide-covered surfaces of Pt, electrodeposited Ni, Co and $Ni_{20}Co_{80}$ alloy through the charge required for monolayer adsorption of the oxygen intermediate species involved in the OER (i.e., overpotential deposited oxygen (OPD O) in 5 M KOH solutions). Note that in the new technique, it is the oxygen species deposited at potentials considerably more anodic to the oxygen evolution potential (i.e., OPD O) that is considered and not the UPD ones mentioned above in the cyclic voltammetric method.

2. Method

The new *in situ* procedure involves galvanostatic charging of an electrode at various current densities for a given period of time followed by direct discharging over a small load. The measurement of the charge, which corresponds to electrochemical desorption of a monolayer of adsorbed OPD O species, is based on the recording and analysis of the discharge current-time transients.

0021-891X

The important assumptions required are as follows: (i) On charging, the charge passed to the electrode is first consumed in the interfacial double-layer (d.l.) charging followed by OPD O adsorption at active oxide surfaces, and that (ii) one atom of OPD O is adsorbed on each metal oxide molecule of the electrode surface lattice. (iii) As the electrode surface reaches a stable, but not necessarily full, coverage by the absorbed intermediate(s) in the high overpotential region, oxygen can then be evolved through electrochemical or chemical desorption of the adsorbed oxygen intermediate species. (iv) When the charged electrode is subjected to a discharge, the previously adsorbed OPD O will undergo spontaneous self-desorption, resulting in a self-discharge current, $i_{OPD,O}$, the magnitude and duration of which depends upon the degree of coverage of the electrode by the OPD O.

The charge corresponding to the desorption, $Q_{OPD,O}$ can be estimated by integration of the discharge current vs time curve. When this charge is plotted for a range of charging currents (or their corresponding steady-state potentials which can be obtained from the potential against log current density relation), an 'S'-shaped curve should be obtained, corresponding to the progressive covering of the electrode surface by the intermediate. Thus, in such a plot, the limiting charge value attained at the 'plateau', after correction for the residual charge, represents precisely the charge required for the formation of monolayer coverage of the adsorbed OPD O intermediate in the OER at the electrode. According to theoretical calculations in the literature [5], the charge needed for full site monolayer coverage of an electrode by the OPD O can be taken as 420 μC cm^{-2}.

3. Experimental details

A glass cell equipped with 3-separated electrode compartments for the working, counter and reference electrode was used. The electrolyte ohmic drop was minimized by the use of a Luggin capillary and was evaluated by a.c. impedance spectroscopy to be between 0.4–1.0 Ω. 5 M KOH solutions were prepared from recrystallized KOH pellets in doubly distilled water. The electrolyte in the working compartment was continuously deaerated and stirred with a flow of prepurified grade nitrogen gas during experiment. A large piece of platinized platinum foil was used as the counter electrode. A Hg/HgO/5 M KOH reversible electrode was used as the reference electrode and the potentials reported here are presented on the reversible hydrogen scale. A short piece of bright platinum wire (Omega, 99.9%), 0.25 mm in diameter, was sealed in glass and used as the platinum test electrode with an exposed area of 0.157 cm^2. Ni and Co electrodes were prepared by electrodeposition on copper wire substrates having an area of approximately 0.2 cm^2 from solutions containing 0.5 M H_3BO_3, 0.5 M Na_2SO_4 and 0.5 M of either $NiSO_4 \cdot 6H_2O$ or $CoSO_4 \cdot 7H_2O$ at room temperature. Plating solutions for $Ni_{20}Co_{80}$ alloy were prepared by mixing equal volumes of the nickel and cobalt plating solutions. All depositions were conducted at a current density of 50 mA cm^{-2} for 15 min. At the end of deposition, the electrode was rinsed thoroughly with water and then air-dried and stored in a desiccator. A set of at least two electrodes of the same kind were prepared and tested for each experiment. Atomic composition at the surface of the alloy was examined by Energy Dispersive Spectroscopy (EDS) and was found to be 20% in Ni and 80% in Co. For each new experiment, the platinum electrode was cleaned, but not polished, by brief immersion of the electrode in a bath of dilute aqua regia solution (1 : 3 HNO_3 : HCl), followed by thorough rinsing with water while as-deposited metals and alloys were used. Double-distilled water was used throughout this study.

The circuit used in this study is shown in Fig. 1. Tafel steady-state polarization and galvanic charging experiments were carried out with a current source (Keithley model 224) in 5 M KOH at 298 K over a range of current densities (0.64 μA to 31.8 mA cm^{-2} apparent area at Pt and about 20 μA to 50 mA cm^{-2} apparent area at Ni, Co and $Ni_{20}Co_{80}$ alloys). The time of polarization at each current density was 30 s for the Tafel experiments and 10 s for the charging experiments. At the end of a charging period, the electrode was discharged immediately through a large counter electrode and a 1 Ω series resistor by means of a micro mercury-wetted contact relay switch (C.P. Clare, HG-1002). The change in discharge current with time was followed as potential across the resistor with a digital oscilloscope (NIC model 204). The procedure was repeated for a range of current densities that was similar to the Tafel experiments. All experiments were conducted in the direction from high to low currents.

A.c. impedance measurements were carried out immediately after each Tafel and charging/discharging

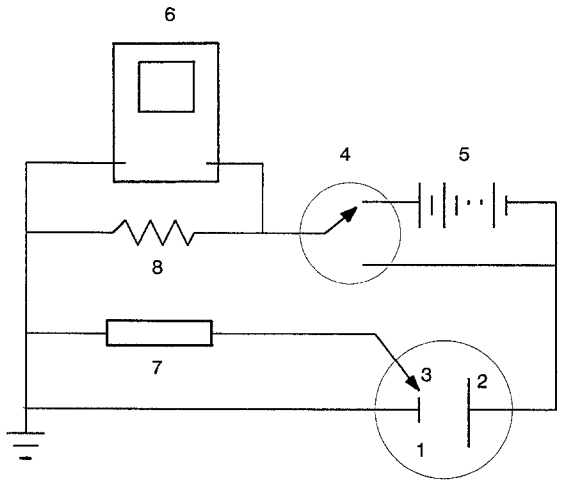

Fig. 1. Basic circuitry used in the charging and discharging experiments: (1) working electrode, (2) counter electrode, (3) reference electrode, (4) mercury relay switch, (5) current source, (6) digital oscilloscope, (7) high impedance electrometer, (8) 1 Ω resistor.

experiment under similar experimental conditions using a computer-controlled PAR 273 potentiostat coupled with a PAR 5208 two phase lock-in analyser. The a.c. impedance of the test electrode was evaluated at several high d.c. level overpotentials over a range of frequencies from 100 000 to 5 Hz. Under such high overpotential conditions, the frequency response of the impedance is mainly that of the charging and discharging of the C_{dl} coupled with the faradaic resistance $R(\eta)$ at an overpotential η. Thus, the C_{dl} can be estimated from the Nyquist real against imaginary semi-circular plots using the basic equation $C_{dl} = (\omega R(\eta))^{-1}$; where ω is the angular frequency in radians at the top of the semicircular plot, and $R(\eta)$ is the resistance measured as the base of the plot. Cyclic voltammograms were recorded using the PAR potentiostat and the NIC oscilloscope at the test electrodes in nitrogen atmosphere in 5 M KOH at room temperature.

4. Results and discussion

4.1. *Steady-state Tafel relations*

Figure 2 shows the overpotential against log (polarizing or charging current density), V against $\log i$, Tafel relation for Pt in 5 M KOH for current densities from 0.64 μA to 31.8 mA apparent cm^{-2} which corresponds to an overpotential change from 0.17 to 0.68 V. A linear low current density region from 0.17 to 0.31 V with a Tafel slope of 37 mV $decade^{-1}$ and a curved high current density region from 0.31 to 0.68 V is observed. This is not a common Tafel behaviour reported for Pt in alkaline solutions (cf., [6]), however, conflicting Tafel relations have been reported in the literature (e.g., [7]). All of these ambiguities probably stem from the different electrode pretreatment procedures leading to various kinds of platinum oxide surfaces. The slopes of the Tafel relations observed here for Pt, however, can be associated with an electrochemical oxide path mechanism with the chemical recombination of OPD O (Equation 3) as the rate determining step [8], that is,

$$\underset{}{OH^- + Pt.ox} \rightleftharpoons \underset{\text{OPD OH}}{Pt.ox.OH(ads)} + e^- \quad (1)$$

$$\underset{\text{OPD OH}}{Pt.ox.OH(ads)} + OH^- \rightleftharpoons \underset{\text{OPD O}}{Pt.ox.O(ads)} + H_2O + e^- \quad (2)$$

$$\underset{\text{OPD O}}{2Pt.ox.O(ads)} \longrightarrow 2Pt.ox. + O_2 \quad (3)$$

where Pt.ox represents the oxidized surface of platinum electrode.

It can be shown [8] that with such a mechanism, a linear Tafel line with a slope $dV/d\log i = 2.3RT/4F$ (i.e., 15 mV at 298 K) is expected at the low current density region when surface coverage by the intermediate is low, followed by a limiting-current high current density region when the coverage approaches unity. It was found that little or no oxygen evolution could be observed in the low current density Tafel region below 0.31 V.

Figure 3 shows the respective Tafel relations for the electrodeposited Ni, Co and $Ni_{20}Co_{80}$ alloy employed in this study. It is seen that the Tafel relations for Ni and Co electrodes are similar to that of Pt, that is, they consist of a linear low current density region followed by a curved high current density region. Thus, the rate determining reaction in the OER at Ni and Co can also be the chemical desorption of the adsorbed OPD O. The $Ni_{20}Co_{80}$ alloys, on the other hand, show a somewhat linear line throughout the whole current density range. This is probably due to extension of the linear low current density region. All Tafel lines exhibit similar linear low-current density region with Tafel slopes in the range of 50 mV $decade^{-1}$. Note that in the construction of these Tafel lines, active areas of the electrodes measured by the new procedure were employed so that relevant comparison could be made.

The experimentally found Tafel slopes for all the metals and alloy studied here seem to be higher than the expected $RT/4F$ for a chemical recombination

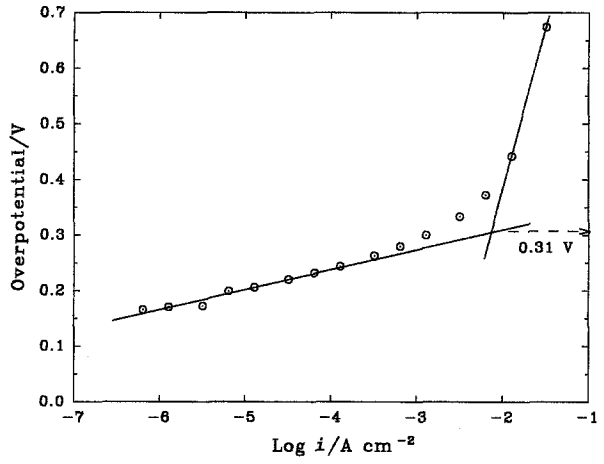

Fig. 2. Log current density *vs* overpotential Tafel relation for the OER at Pt in 5 M KOH at 298 K.

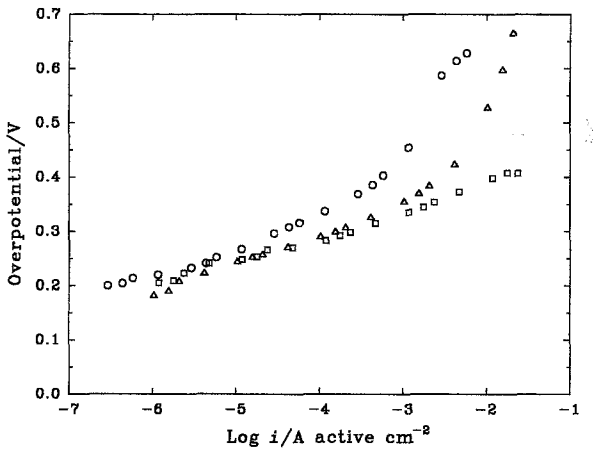

Fig. 3. Log current density *vs* overpotential Tafel relation for the OER at electrodeposited cobalt (○), nickel (△) and $Ni_{20}Co_{80}$ (□) in 5 M KOH at 298 K.

Table 1. Summaries of Tafel slope, electrode roughness, r^*, oxide formation potential and i, $\eta = 0.4$ for Pt, electrodeposited Ni, Co and $Ni_{20}Co_{80}$ in 5 M KOH at 298 K

Material	*Pt*	*$Ni_{20}Co_{80}$*	*Ni*	*Co*
Tafel slope*/mV dec^{-1}	36 ± 8	40 ± 5	54 ± 4	67 ± 13
(a) Roughness by a.c. impedance	1.3 ± 0.2	24 ± 1	19 ± 2	756 ± 6
(b) Roughness by OPD O	3.1 ± 0.1	17 ± 2	7 ± 1	91 ± 7
$r^* = (b)/(a)$	2.4 ± 0.5	0.69 ± 0.1	0.37 ± 0.1	0.12 ± 0.0
Oxide formation potential/V	1.0	1.36	1.39	1.50
$i_{\eta=0.4}$†/A cm^{-2}	1.0×10^{-2}	1.0×10^{-2}	4.2×10^{-3}	6.6×10^{-4}

* taken in the low current density linear regions of the Tafel lines.
† $i_{\eta=0.4}$ represents the current measured at an overpotential of 0.4 V.

control mechanism. These are listed in Table 1. The minor differences observed here can be attributed to the fact that the surface of an oxide electrode should never be treated merely as an electron sink, as was assumed in reference [8], but one that is actively involved in the OER process. For example, the Ni^{4+} and Co^{4+} higher oxidation states in the film surfaces of oxidized Ni and Co can act as mediator for the OER (see Equations 7 and 8) as was proposed by Conway [10]. Mediation of the OER by Pt^{4+} is not as likely as in the baser metal but slight involvement of the high oxidation state, particularly at high overpotentials, should not be excluded altogether.

4.2. *Discharge current against time transients*

Figure 4 shows a series of four digitally acquired $i_{OPD,O}$ discharge current density against time transients for four prior *anodic* charging current densities (not shown in figure) of 3.18 μA, 31.8 μA, 318 μA, and 31.8 mA apparent cm^{-2} at Pt in 5 M KOH. As the electrode was subject to a discharge, a *cathodic* current was recorded, the magnitude of which was many times larger than that of prior charging current. This discharge current diminishes at first rapidly then slowly to zero current in less than 16 ms depending on the magnitude of the charging current. Similar effects, but in the opposite direction, were observed when cathodic charging is used (cf. [4]). Figure 5 compares two discharge current transients at Pt: one obtained using a prior anodic charging current of 0.64 mA apparent cm^{-2} and the other, a prior cathodic charging current of -0.64 mA apparent cm^{-2}. Note that prior anodic charging resulted in cathodic discharge current and vice versa for the cathodic charging process. The observed change of sign in the discharge current is, however, expected since the electrochemical process giving rise to the discharge current is the self-discharge of the adsorbed intermediates, which is a reduction process in the case of the OPD O species but an oxidation one in the case of the OPD H. At Pt, namely,

(I) two-electron self-discharging of Pt.ox.O in 5 M KOH

$$\underset{\text{OPD O}}{\text{Pt.ox.O(ads)}} + H_2O + e^- \xrightarrow{\text{discharging}} \underset{\text{OPD OH}}{\text{Pt.ox.OH(ads)}} + OH^- \quad (4)$$

$$\underset{\text{OPD OH}}{\text{Pt.ox.OH(ads)}} + e^- \xrightarrow{\text{discharging}} \text{Pt.ox.} + OH^- \quad (5)$$

(II) one-electron self-discharging of PtH in 5 M KOH

$$\underset{\text{OPD H}}{\text{PtH(ads)}} + OH^- \xrightarrow{\text{discharging}} Pt + H_2O + e^- \quad (6)$$

Similar discharge current behaviours were also observed at Ni, Co and $Ni_{20}Co_{80}$ alloys surfaces. However, there are fundamental differences between the origins of the adsorbed oxygen species at Pt and

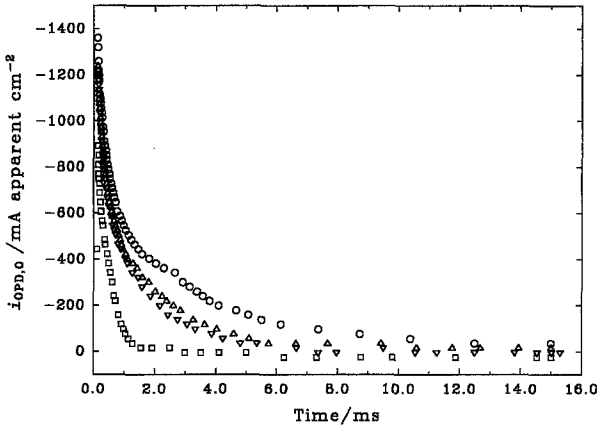

Fig. 4. Four discharge current density *vs* time curves for four prior anodic charging current densities of 31.8 mA (○), 3.18 mA (△), 318 μA (▽) and 31.8 μA (□) apparent cm^{-2} at Pt in 5 M KOH.

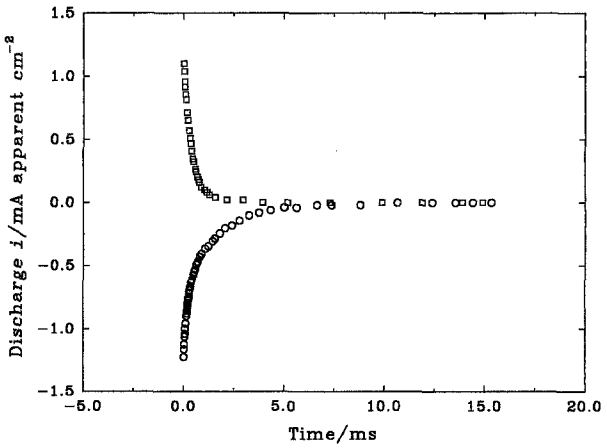

Fig. 5. Same as in Fig. 4 but for the prior charging current densities of -0.64 mA apparent cm^{-2} (□) and $+0.64$ mA apparent cm^{-2} (○).

that at the base metals. On the surfaces of Ni, Co and their alloys, oxygen evolution is known to proceed on a three-dimensional, thick oxide film (e.g., Ni.O.OH) on which the processes of OPD OH discharge take place [8, 9] whereas on Pt, oxygen is evolved on a thin, monolayer thick, oxide film. In addition, mixed-oxidation-states surface species can be developed at the surfaces of the base metal electrodes as potential is changed, e.g., Ni^{3+}/Ni^{4+}, corresponding to adsorption of OH intermediate species at the surface. Therefore, the oxidation state of the surface oxide is believed to be involved in the mechanism of the evolution reaction, possibly via the following steps [10]: (III) Adsorption of intermediate species below full or some stable coverage,

$$\underset{\text{hydrous Ni bulk oxide}}{Ni^{3+}.O.OH} + OH^- = \underset{\substack{\text{absorbed OH}\\ \text{surface intermediate}\\ \text{OPD OH(ads)}}}{Ni^{4+}.O.O} + H_2O + 2e^- \quad (7)$$

(IV) Oxygen evolution at appreciable high polarization via chemical desorption of two OPD OH(ads) species,

$$\underset{\text{OPD OH(ads)}}{2Ni^{4+}.O.O} + H_2O = 2Ni^{3+}.O.OH + \tfrac{1}{2}O_2 \quad (8)$$

Upon termination of polarization, oxygen evolution continues while the electrode undergoes self-relaxation possibly via Equation 8 and suffers a decrease in oxidation state until the electrode potential is the same as that of the reversible potential of the OER or some other stable value. This mode of OPD OH(ads) desorption is relatively slow (chemical recombination) when compared to that of OPD OH electrochemical desorption (reverse of Equation 7). Thus, when a polarized electrode is made to be discharged through a large counter electrode and a small series resistor, as in the simple discharge procedure employed here, electrochemical desorption prevails.

4.3. *$Q_{OPD.O}$ against V relation derived from a series of $i_{OPD.O}$ against t transients*

As stated earlier, the quantity of electrochemical species, OPD O, that is formed and adsorbed on the electrode surface during charging can be estimated by integration of the $i_{OPD,O}$ discharge current against time curve (i.e., $Q_{OPD,O}$). Figure 6 shows the dependence of $Q_{OPD,O}$ as a function of the steady-state overpotential, which correspond to a range of prior charging current densities i, for the Pt system in 5 M KOH. It is seen that the charge increases quickly from a residual value of 86 μC apparent cm^{-2} at 0.2 V to a limiting value of $\sim$1365 $\mu C\,cm^{-2}$ at $\sim$0.27 V. This charge limit or 'plateau' spans over a range of overpotentials from 0.27 to 0.33 V having a mean value at 0.31 V. On further increase in overpotential, the charge increases gradually without reaching a limit (most likely due to three-dimensional oxide growth).

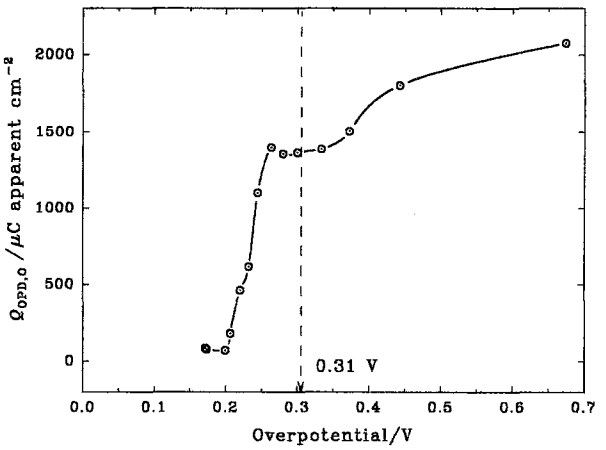

Fig. 6. Charge *vs* overpotential plot derived from a series of discharge current *vs* time curves for a series of prior charging current densities for Pt in 5 M KOH.

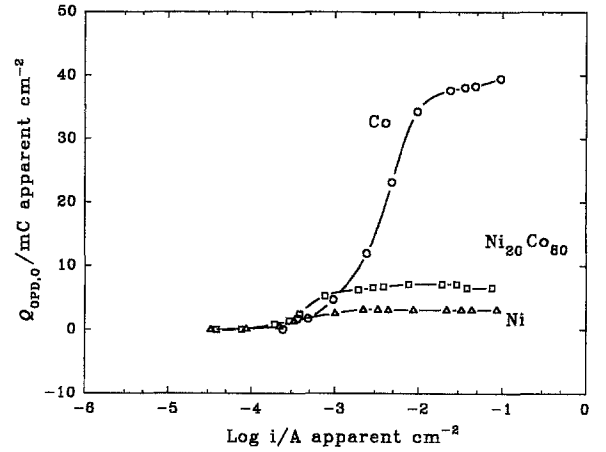

Fig. 7. Same as in Fig. 6 but for Co, Ni and $Ni_{20}C_{80}$.

From Fig. 6, it is evident that all $Q_{OPD,O}$ charges occurred at potentials well above the overpotential of 0.2 V. Thus, one can assume that the adsorbed species which gave rise to the discharge current was one deposited at an overpotential. Since no surface oxide or molecular oxygen can be reduced in this high overpotential range, the species could only be the adsorbed intermediates involved in the OER.

In Fig. 7, for the sake of convenience, the $Q_{OPD,O}$ against $\log i$ plots rather than the $Q_{OPD,O}$ against V relations for Ni, Co and $Ni_{20}Co_{80}$ are compared because these materials exhibit different steady-state Tafel relations. Unlike Pt, only simple 'S'-shaped $Q_{OPD,O}$ against $\log i$ curves were obtained from these base metals and alloy, that is, once the plateau has been attained, no further increase in charge was observed with increasing potential.

4.4. *Relationship between Tafel relations and the $Q_{OPD,O}$ against V or log i plots*

It is to be recalled that in Section 2, the oxide electrode is assumed to be progressively covered by the reaction intermediate as the charge passed to the electrode increases. Not until the surface is saturated by the adsorbed species, that is, full or stable coverage, molecular gas evolution will not occur. This assumption

is confirmed experimentally in the present study and a close relationship exists between the OER Tafel relation and the $Q_{OPD,O}$ against V plot of Pt, as was observed previously also for the HER Tafel relation and the $Q_{OPD,H}$ against V plot [4]. That is, the potential at which the low current density linear Tafel region (in which no oxygen gas is evolved, as shown in the cyclic voltammogram of Pt, Fig. 8) ends matches well the potential of the 'plateau' in the $Q_{OPD,O}$ against V plot, 0.31 V (compare Fig. 2 and Fig. 6). It was reasonable therefore that in the low current density region of the OER Tafel relations, the coverage of electrode by the intermediate OPD O(ads) is low and is approaching full coverage or some stable value at 0.31 V.

Although not as clear as at Pt, all the $Q_{OPD,O}$ against $\log i$ plots for the base metals and their alloy are related to their Tafel relations, that is, the $\log i$ value at the end of the low current Tafel regions matches that of the plateau (i.e., −2). In the case of Ni, the species giving rise to the plateau in the charge against $\log i$ plots is most likely that of the Ni^{4+}.O.O (equivalent to the OPD OH species at Ni). Since no higher oxidation state is possible under the experimental conditions, no further increase in charge is observed. In the case of Co or $Ni_{20}Co_{80}$ alloy, similar type of adsorbed species in a form of Co^{4+}.O.O [11] for the former and a mixture of Co^{4+}.O.O and Ni^{4+}.O.O for the latter is expected as the potential of the electrode is made more positive than the reversible potential of the OER. The above assumption is supported by the Pourbaix diagram of Ni and Co in which Ni^{4+} and Co^{4+} are the stable species at high potentials in alkaline pH.

4.5. *Electrode area by a.c. impedance and OPD O adsorption/desorption technique*

Electrode areas at Pt and the base metals and their alloys were estimated by the a.c. impedance and the OPD O adsorption/desorption methods under similar experimental conditions. Active area estimation for the Pt oxide electrode by the OPD O method is rather simple and straightforward. That is, the charge required for one monolayer coverage of 1 cm^2 of the electrode surface is taken as 420 μC (based on 2 electrons per oxide molecule on the surface, see Equations 4 and 5). From Equation 7, again two electrons are involved in the production of each adsorbed intermediate for Ni oxide. Thus, logically, 420 μC is necessary to achieve full coverage on 1 cm^2 of the oxide of Ni, that of Co, and that of their alloys as well. It is understood that the adsorption process on the base metals might not be limited to the surface but also extend slightly inside the immediate surface region of the electrode. Providing that such penetration can be ignored and that the adsorption of these NiO.O intermediates on the electrode surface is a one to one process, that is, one OH(ads) to each surface Ni hydrous oxide molecule, the surface area measurement procedure by the adsorption/desorption of such species is still valid. For the a.c. impedance data, 40 $\mu F\,cm^{-2}$ is taken as the double-layer capacitance for smooth [12] oxide covered electrodes. Table 1 summarizes the different values obtained for the oxide-covered Pt, Ni, Co, and $Ni_{20}Co_{80}$ electrodes in 5 M KOH at ambient temperature.

It is evident from Table 1 that electrode roughness (taken as the ratio of the real or active area to that of geometrical) estimated by the OPD O adsorption/desorption method are in the same order of magnitude as those from the a.c. technique except for cobalt oxide. The high roughness found for Co oxide by the a.c. method could not be due to any pseudo-capacitance of the oxide film, C_ϕ, since only high d.c. polarization potentials were used in the a.c. measurements; consequently $C_{dl} \gg C_\phi$. The most probable reason for the observed differences in the case of cobalt is the fact that a.c. impedance estimates the total available surface area at the oxide electrode surface, regardless of whether it is active for the reaction of interest or not. On the contrary, the adsorption/desorption method detects species which are adsorbed on the surface of the oxide electrode; therefore, surfaces which are not catalytically active for such an adsorption would be ignored. That is, surface area measured by the adsorption/desorption technique is not just real but also active for the reaction under consideration, in this case the OER.

Hence, it is fair to assume that the ratio of the electrode roughness given by the adsorption/desorption method to that of by the a.c. impedance technique (r^*) is a good indication of the activity of the oxide surface towards the OER. Thus, Pt, having a ratio of 2.4, is supposedly most active for the OER followed by $Ni_{20}Co_{80}$ (0.69), Ni(0.37) and Co(0.12), so that the Ni–Co alloy is more active than either of its parent metals. This is in good agreement with the order of activity for the OER for these metals commonly reported in the literature (e.g., [13–15]). The fact that r^* for Pt is greater than unity cannot be accounted for easily since it would imply that the active surface area on this material is actually larger than its real surface. One explanation for the observed discrepancy would be that of charge contribution

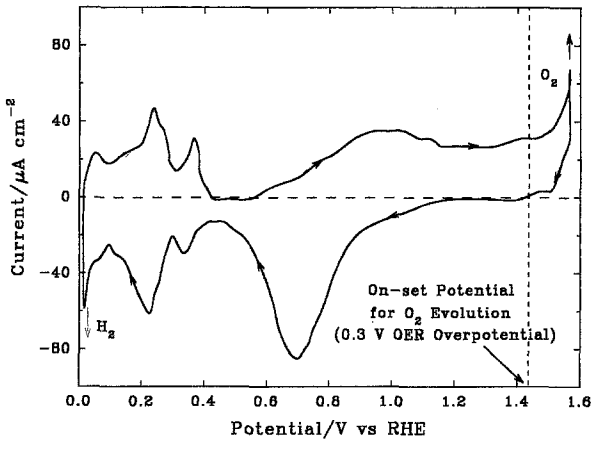

Fig. 8. Typical cyclic voltammogram for Pt in 5 M KOH at 298 K at a sweep rate of 50 mV s^{-1}.

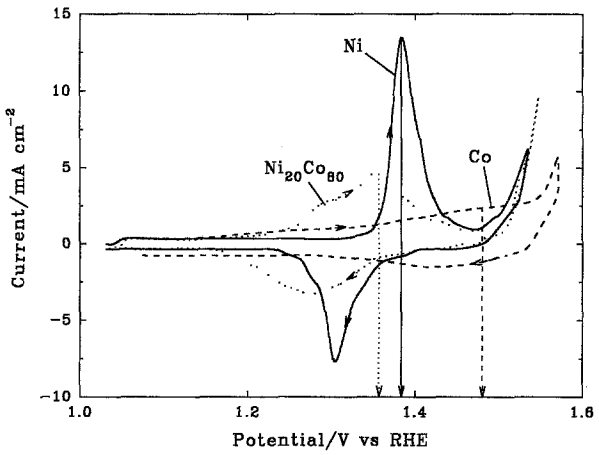

Fig. 9. A series of three cyclic voltammogram for Ni, Co and $Ni_{20}Co_{80}$ in 5 M KOH at 298 K. Sweep rate = 50 mV s^{-1}.

from absorbed OPD O species inside the metal matrix, however, this is not supposed to take place, at least in noble metals such as Pt. The greater than unity comparison of the OPD O with a.c. impedance results, however, can be explained by the following: (i) the precise charge formally required for full monolayer coverage of a square centimetre of electrode surface is uncertain. The theoretical value of 420 μC cm^{-2} for a two-electron OPD O adsorption process was served only as a universal accepted reference; and (ii) the selected value of $C_{dl} = 40\,\mu$F cm^{-2} for oxide covered electrodes is also questionable. Thus, it is not surprising that some of the r^* values are greater than unity but the comparison is quite valid on a relative basis.

The above claim that Ni–Co is more active than Ni and Co for the OER is further supported by their steady-state polarizations and cyclic voltammograms. In Fig. 3, at a relatively high oxygen overpotential of 0.4 V, the observed current densities (current real cm^{-2}, see Table 1) for the OER was found to be in the order $Ni_{20}Co_{80}$ > Ni > Co. From the respective cyclic voltammograms of $Ni_{20}Co_{80}$, Ni and Co in Fig. 9, it can be seen that the potential for the metal oxide formation increases in the order $Ni_{20}Co_{80}$, Ni, Co. This is consistent with the fact that the processes of OPD O adsorption and oxygen evolution should not take place until the electrode surface is covered by a film of oxide; consequently, the lower is the oxide formation potential, the lower is the onset potentials for the OPD O adsorption process and, ultimately the easier it is for oxygen to evolve.

5. Conclusions

The overpotential-deposited oxygen species involved in the OER mechanism steps could be detected and measured by the adsorption/desorption technique. On most of the metals studies, the area derived from the monolayer coverage by the adsorbed intermediates was found to be similar to that from the a.c. impedance method. The order of activity for the adsorption of OPD O was found to be Pt > $Ni_{20}Co_{80}$ > Ni > Co. This is consistent with the commonly reported fact that NiCo is more active than its parent metals for the OER.

References

[1] S. Trasatti, *in* 'Advances in Electrochemical Science and Engineering', vol 2, (edited by H. Gerischer and C. W. Tobias), VCH Press, Weinheim (1992) p. 1.
[2] H. Angerstein-Kozlowska, *in* 'Comprehensive Treatise of Electrochemistry', vol. 9 (edited by E. Yeager, J. O'M Bockris, B. E. Conway and S. Sarangapani), Plenum Press, NY (1984) p. 15.
[3] A. T. Kühn, 'Techniques in Electrochemistry, Corrosion, and Metal Finishing', John Wiley & Sons, New York (1987) p. 3.
[4] J. C. K. Ho and D. L. Piron, *J. Electrochem. Soc.* **142** (1995) 1144.
[5] A. I. Fedorova and A. N. Frumkin, *J. Phys. Chem. USSR* **27** (1953) 247.
[6] B. E. Conway and T. C. Liu, *Langmuir* **6** (1990) 268.
[7] A. Damjanovic, A. Dey, and J. O'M. Bockris, *Electrochim. Acta* **11** (1966) 791.
[8] J. O'M. Bockris, *J. Chem. Phys.* **24** (1956) 817.
[9] B. E. Conway and T. C. Liu, *J. Chem. Soc., Faraday Trans. 1* **83** (1987) 1063.
[10] B. E. Conway and P. L. Bourgault, *Can. J. Chem.* **37** (1959) 292.
[11] B. E. Conway and T. C. Liu, *Ber. Bunsenges. Phys. Chem.* **91** (1987) 461.
[12] A. N. Frumkin, *J. Res. Inst. Catalysis* (Hokkaido Univ.) **15** (1967) 61.
[13] J. Haenen, W. Visscher and E. Barendrecht, *Electrochim. Acta* **31** (1986) 1541.
[14] I. A. Raj and K. I. Vasu, *J. Appl. Electrochem.* **20** (1990) 32.
[15] L. Brossard, *Int. J. Hydrogen Energy* **18** (1993) 455.